Eur. Phys. J. B **44**, 41–45 (2005)
DOI: 10.1140/epjb/e2005-00097-3

THE EUROPEAN PHYSICAL JOURNAL B

Rainbows in transmission of high energy protons through carbon nanotubes

S. Petrović[a], D. Borka, and N. Nešković

Laboratory of Physics (010), Vinča Institute of Nuclear Sciences, PO Box 522, 11001 Belgrade, Serbia and Montenegro

Received 3 December 2004 / Received in final form 17 January 2005
Published online 16 April 2005 –

Abstract. We investigate theoretically the angular distribution and the rainbows in the case of 1 GeV protons transmitted through the 1 μm long rope of (10, 10) single-wall carbon nanotubes. The angular distribution of transmitted protons is generated by the computer simulation method using the numerical solution of the proton equations of motion. Then, the rainbow lines corresponding to the angular distribution are determined. The analysis shows that the rainbow pattern defines the angular distribution – all its pronounced maxima except the maximum lying at the origin are the rainbow maxima. A possible application of the rainbow effect for characterization of nanotubes is suggested.

PACS. 78.70.-g Interactions of particles and radiation with matter – 61.85.+p Channeling phenomena (blocking, energy loss, etc.) – 78.67.Ch Nanotubes – 02.40.-k Geometry, differential geometry, and topology

1 Introduction

Carbon nanotubes were discovered in the beginning of 1990s, by Iijima [1]. They can be described as sheets of carbon atoms lying at the (two-dimensional) hexagonal lattice sites rolled up into cylinders [2]. Their diameters are of the order of a nanometer and they can be more then a hundred micrometers long. A single-wall nanotube is formed from one sheet only. Thanks to their remarkable geometrical and physical properties [2], nanotubes are considered to be the basic elements in the newly developing field of nanoelectronics [3].

Soon after the discovery of nanotubes, the effect of channeling of positively charged particles in them was foreseen and a new source of hard X-rays, emitted by the channeled particles, was discussed [4]. After that, a number of theoretical groups has studied ion channeling in nanotubes [5–8]. The main objective of those studies was to investigate the possibility of guiding high energy ion beams with bent nanotubes. Greenenko and Shulga [8] investigated in detail the ion motion through the straight and bent nanotubes taking into account the azimuthal variation of the interaction potential. The other groups [5–7] used the azimuthally averaged interaction potential. It should be noted that no ion channeling experiment with nanotubes has been carried out so far, mainly due to the problem of preparation of the sample.

It is well known that meteorological rainbows appear as a consequence of photon scattering from water droplets. However, it has been established that rainbows occur also and play important roles in nucleus-nucleus collisions, atom or ion collisions with atoms or molecules, electron-molecule collisions, atom or electron scattering from crystal surfaces, and ion channeling in crystals. Recently, the theory of crystal rainbows was formulated, as the proper theory of ion channeling in thin crystals [9]. It has been demonstrated that the rainbow patterns ensure the full explanation of the angular distributions of ions transmitted through channels of thin crystals [9–11].

2 Theory

From the point of view of ion channeling a nanotube is very short if the majority of ions make before leaving it less than one quarter of an oscillation around the channel axis, it is short if they make between one quarter of an oscillation and a few oscillations, and it is long if they make more than a few oscillations [9,10]. If the nanotube is very short, the angular distribution of transmitted ions is dominated by the rainbow effect, and it is easy to deduce the structure of the nanotube from it. If the nanotube is short, the angular distribution is still dominated by the rainbow effect, but the deduction of the structure of the nanotube is harder. However, if the nanotube is long, the rainbow effect becomes smeared out, and the deduction of the structure of the nanotube becomes very hard. This smearing out appears primarily as a consequence of the uncertainty of the ion scattering angle caused by its collisions with the nanotube electrons [12].

In this article we describe the rainbows and the angular distribution of 1 GeV protons transmitted through

[a] e-mail: petrovs@vin.bg.ac.yu

the 1 μm long (10, 10) single-wall carbon nanotubes. These nanotubes are achiral – they consist of the atomic strings parallel to their axes. It is assumed that the nanotubes form a rope whose transverse cross section can be described via a (two-dimensional) hexagonal superlattice with one nanotube per lattice point [13]. The aim of the study is to show that the theory of crystal rainbows can be applied successfully to the transmission of protons through the rope, and that the rainbow pattern provides the full explanation of the angular distribution of transmitted protons.

We chose first the rope length (1 μm), to have a sample that could be prepared using the existing techniques. Then, we chose the ion species and energy (1 GeV protons), to have the projectiles that can be delivered routinely using the existing accelerators, and to make the rope very short.

The system we investigate is a proton moving through a rope of nanotubes. It is assumed that the interaction of the proton and the rope is elastic and that it can be treated classically [14]. The z axis coincides with the rope axis and the origin lies in its entrance plane. The initial proton velocity vector, $\mathbf{V}_0$, is taken to be parallel to the rope axis. However, the theory we apply can be extended easily to the case in which the angle between variable $\mathbf{V}_0$ and the rope axis is not equal to zero [9].

We take that the interaction potential of the proton and a nanotube atom is of the Thomas-Fermi type and adopt for it the Molière's expression [5,8,9],

$$V(r) = \left(Z_1 Z_2 e^2/r\right)[0.35\exp(-br) + 0.55\exp(-4br) + 0.10\exp(-20br)], \quad (1)$$

where Z_1 and Z_2 are the atomic numbers of the proton and the atom, respectively, r is the distance between the proton and the atom, $b = 0.3/a$, $a = [9\pi^2/(128Z_2)]^{1/3}a_0$ is the screening radius of the atom, and a_0 is the Bohr radius. It has been proven that this expression provides excellent agreement with experimental results in the field of ion channeling [15]. We also assume that we can apply the continuum approximation [14], i.e., that the potential of an atomic string of a nanotube can be approximated with its average along the rope axis. The continuum potential of the rope is the sum of the continuum potentials of the atomic strings of the nanotubes. This potential determines, through the Poisson equation, the electron density in the rope averaged along its axis. We take into account the thermal vibrations of the nanotube atoms [9]. However, we neglect the proton energy loss and the uncertainty of the proton scattering angle caused by its collisions with the nanotube electrons, and take that the proton can not capture the nanotube electrons. These approximations are justified by the fact that the rope is very short [9,12].

In order to obtain the components of the proton scattering angle, Θ_x and Θ_y, one has to solve the proton transverse equations of motion, and use expressions $\Theta_x = V_x/V_0$ and $\Theta_y = V_y/V_0$, where V_x and V_y are the transverse components of the final proton velocity vector, $\mathbf{V}$. Since the potential of the rope is continuous, the solution of the proton longitudinal equation of motion is trivial. The chosen proton velocity requires the use of the relativistic transverse equations of motion. The only change in these equations with respect to the non-relativistic ones is the appearance of the relativistic proton mass instead of its rest mass. The proton longitudinal motion is relativistic but its transverse motion is not. The angular distribution of transmitted protons is generated by the computer simulation method.

Transmission of the protons through the rope is a scattering process that can be analyzed via the corresponding mapping of the impact parameter plane, the xy plane, to the scattering angle plane, the $\Theta_x\Theta_y$ plane [9]. Since the proton scattering angle is small (much smaller then the critical angle for channeling), its differential transmission cross section is given by expression $\sigma = 1/|J|$, where $J = \partial_x\Theta_x\partial_y\Theta_y - \partial_x\Theta_y\partial_y\Theta_x$ is the Jacobian of the mapping of the impact parameter plane to the scattering angle plane [9].

Thus, the rainbow lines in the impact parameter plane, i.e., the lines along which the proton differential transmission cross section is singular, are determined by equation $J = 0$. The rainbow lines in the scattering angle plane are the images of the rainbow lines in the impact parameter plane defined by the corresponding mapping of the impact parameter plane to the scattering angle plane. These lines separate the bright regions of the scattering angle plane from its dark regions.

The bond length of two nanotube atoms is 0.14 nm [2] and, hence, the diameter of a nanotube is 1.34 nm. The distance between the centers of two neighboring nanotubes is 1.70 nm [13]. The one-dimensional thermal vibration amplitude of the nanotube atoms is estimated, using the Debye approximation, to be 0.0053 nm [16].

In the case we analyze the nanotube walls define two separate regions in the transverse plane: inside the nanotubes and in between them. In accordance with this, the rope is characterized by two types of channels: the circular one, whose center coincides with the center of the region inside each nanotube, and the triangular one, whose center coincides with the center of the region in between each three neighboring nanotubes. The primitive cell of the hexagonal superlattice is a rhomb defined by each four neighboring nanotubes. This is seen clearly in Figure 1. In analogy with ion channeling in crystals [9,10], one can define two characteristic frequencies of the proton motion in the transverse plane, corresponding to the protons moving close to the centers of the circular and triangular channels. The two frequencies can be determined from the second order terms of the Taylor expansions of the continuum potential of the rope in the vicinities of the centers of the two types of channels. Also, one can define the reduced rope length, $\Lambda = fL/V_0$, where V_0 is the initial proton velocity, L the rope length and f the frequency of transverse proton motion close to the channel center. The values of variable Λ equal to 0, 0.5, 1, ... correspond to the beginnings of the cycles of the angular distribution of transmitted protons, which are called the rainbow cycles [9,10]. Consequently, there are two reduced

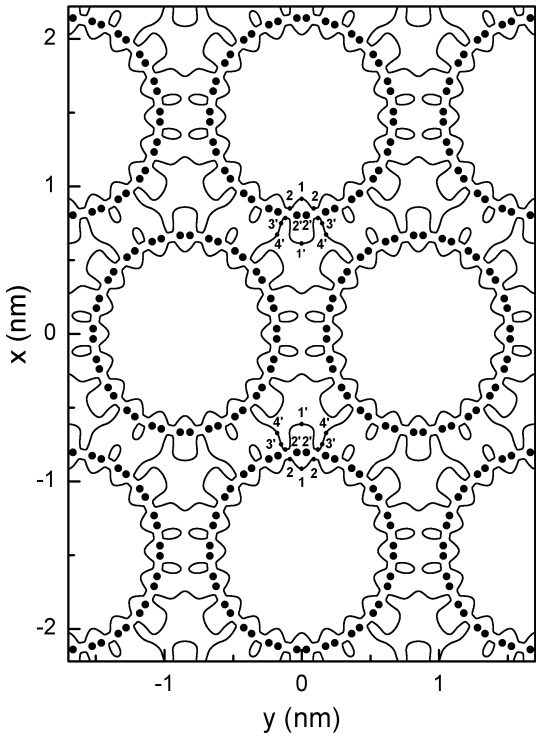

Fig. 1. The rainbow lines in the impact parameter plane for 1 GeV protons transmitted through the 1 μm long (10, 10) single-wall carbon nanotubes.

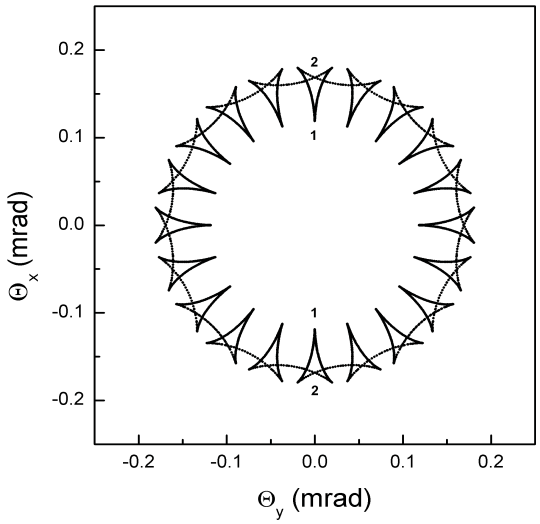

Fig. 2a. The rainbow line in the scattering angle plane corresponding to the rainbow line in the impact parameter plane shown in Figure 1 lying inside each nanotube.

rope lengths, Λ_1 and Λ_2, corresponding to the proton motions close to the centers of the circular and triangular channels, respectively. In the case in question $\Lambda_1 = 0.015$ and $\Lambda_2 = 0.070$. These values tell us that in both cases the majority of protons make before leaving the rope less then one quarter of an oscillation around the channel center (Λ_1, $\Lambda_2 < 0.25$). Therefore, we can say that the rope we investigate is very short [9,10].

The proton transverse equations of motion are solved numerically. The components of the proton impact parameter are chosen uniformly within the primitive cell of the hexagonal superlattice. The proton whose impact parameter is chosen inside one of the circles around the nanotube atoms of the radius equal to the screening radius is disregarded since its scattering angle would be large and it would not undergo the channeling process. As a result, we disregard the collisions that can lead to nuclear and elementary particle reactions. The number of transmitted protons is 2,142,538. The rainbow lines in the impact parameter plane are generated numerically too.

3 Results and discussion

Figure 1 shows the rainbow lines in the impact parameter plane. One can observe that inside each nanotube, i.e., inside each circular channel, there is one (closed) rainbow line while in between each three neighboring nanotubes, i.e., inside each triangular channel, there are one larger and four smaller (closed) rainbow lines.

Figure 2a shows the rainbow line in the scattering angle plane that is the image of the rainbow line in the impact parameter plane lying inside each nanotube. It consists of 20 connected cusped triangular lines lying along the lines $\Phi = \tan^{-1}(\Theta_y/\Theta_x) = 2(n+1)\pi/20$, $n = 0-19$, which correspond to the parts of the rainbow line in the impact parameter plane in front of the 20 pairs of atomic strings defining the nanotube (see Fig. 1). Points 1 and 2 are the intersection points of the rainbow line in the scattering angle plane with the line $\Theta_y = 0$. Points 1 are the apices of the cusps and points 2 are the intersections of the parts of the rainbow line. The corresponding points in the impact parameter plane are designated also by 1 and 2 (see Fig. 1).

The rainbow lines in the scattering angle plane that are the images of the rainbow lines in the impact parameter plane lying in between each four neighboring nanotubes are shown in Figure 2b. The analysis shows that the rainbow pattern consists of two cusped equilateral triangular rainbow lines in the central region of the scattering angle plane with the cusps lying along the lines $\Phi = 2n\pi/3$ and $\Phi = (2n+1)\pi/3$, $n = 0-2$, each connected with three pairs of cusped triangular rainbow lines lying along the same lines, and eight cusped triangular rainbow lines lying in between the six pairs of triangular lines. The two equilateral triangular lines each connected with the three pairs of triangular lines are the images of the two larger rainbow lines while the eight triangular lines are the images of the eight smaller rainbow lines in the impact parameter plane (see Fig. 1). Points $1'$, $2'$, $3'$ and $4'$ are the intersection points of the rainbow lines in the scattering angle plane with the line $\Theta_y = 0$. Points $1'$ are the apices of the cusps and points $2'$, $3'$ and $4'$ are the intersections of the parts of the larger rainbow lines. The corresponding points in the impact parameter plane are designated also by $1'$, $2'$, $3'$ and $4'$ (see Fig. 1).

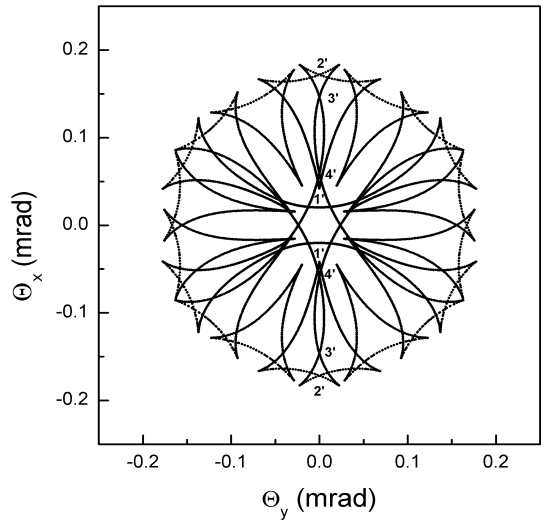

Fig. 2b. The rainbow lines in the scattering angle plane corresponding to the rainbow lines in the impact parameter plane shown in Figure 1 lying in between each four neighboring nanotubes.

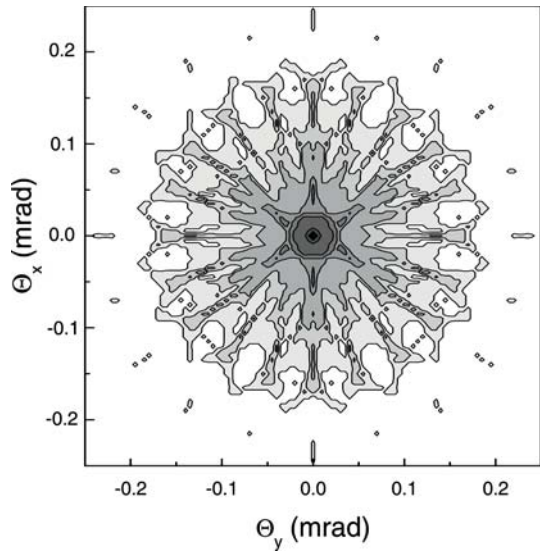

Fig. 3a. The angular distribution of 1 GeV protons transmitted through the 1 μm long (10, 10) single-wall carbon nanotubes. The areas in which the yields of transmitted protons are larger than 0.13, 0.26, 0.39, 1.3, 2.6, 3.9, 13, 26, 39% of the maximal yield are designated by the increasing tones of gray color.

Figure 3a shows the angular distribution of transmitted protons. The areas in which the yields of transmitted protons are larger then 0.13, 0.26 and 0.39%, 1.3, 2.6 and 3.9%, and 13, 26 and 39% of the maximal yield are designated by the increasing tones of gray color. We have chosen these three groups of boundary yields, spanning two orders of magnitude of the yield of transmitted protons, to point out clearly three different parts of the angular distribution. At the very low level of the yield, corresponding to the boundary yields of 0.13, 0.26 and 0.39% of the maximal yield, there are 20 triangular forms in the peripheral region of the scattering angle plane, with the maxima lying on the lines $\Phi = 2(n+1)\pi/20$, $n = 0-19$. Further, at the low level of the yield, corresponding to the boundary yields of 1.3, 2.6 and 3.9% of the maximal yield, there is a hexagonal structure in the central region of the scattering angle plane, with the maxima lying on the lines $\Phi = n\pi/3$, $n = 0-5$. Finally, at the high level of the yield, corresponding to the boundary yields of 13, 26 and 39% of the maximal yield, there is a pronounced maximum at the origin. The analysis shows that the first part of the angular distribution is generated by the protons with the impact parameters close to the atomic strings defining the nanotubes – the 20 triangular forms correspond to the 20 pairs of atomic strings defining each nanotube. The second part of the angular distribution is generated by the protons with the impact parameters in between the nanotubes but not close to the centers of the triangular channels. The third part of the angular distribution is generated to a larger extent by the protons with the impact parameters close to the centers of the circular channels and to a smaller extent by the protons with the impact parameters close to the centers of the triangular channels. It should be noted that most of the protons that generate the third part of the angular distribution, i.e., the maximum at the origin, interact with the nanotubes very weakly – they move through the space inside the nanotubes virtually as through a drift space. Thus, we can say that the angular distribution contains the useful information on the transverse lattice structure of the rope. Its first part (the peripheral region of the scattering angle plane) gives the information on the individual nanotubes while its second part (the central region of the scattering angle plane) gives the information on the way they are connected to each other.

The comparison of Figures 2a and b with Figure 3a clearly shows that the shape of the rainbow pattern determines the shape of the angular distribution. Also, each maximum of the angular distribution, except the maximum lying at the origin, can be attributed to one of the above mentioned characteristic rainbow points in the scattering angle plane. Thus, one can conclude that the rainbow pattern provides the full explanation of the angular distribution.

Figure 3b gives the low and very low levels of the yield of transmitted protons along the line $\Theta_y = 0$. The arrows indicate the above mentioned characteristic rainbow points in the scattering angle plane. It is evident that the two maxima at the low level of the yield can be explained by points $1'$ and $4'$ in the scattering angle plane, and the two shoulders at the very low level of the yield by points 1, 2, $2'$ and $3'$. This means that the characteristic rainbow points in the scattering angle plane could provide information on the continuum potential of the rope at the corresponding points in the impact parameter plane, and, hence, on the average electron density in the rope at these points (see Fig. 1). The two maxima at the low level of the yield can be used to measure the average electron density at points $1'$ and $4'$, lying in between the nanotubes, while the two shoulders at the very low level of the yield can be

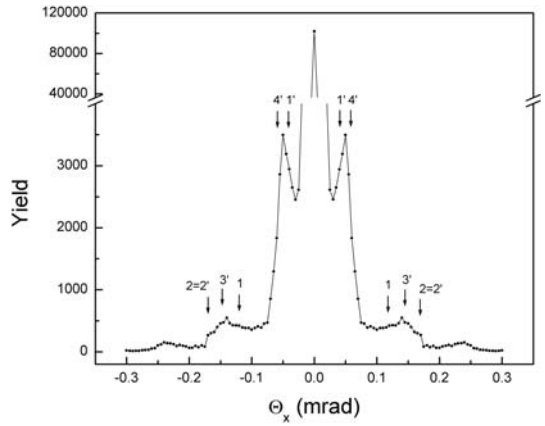

Fig. 3b. The yield of 1 GeV protons transmitted through the 1 μm long (10, 10) single-wall carbon nanotubes along the line $\Theta_y = 0$.

used to measure the average electron density at points 1 and 2, lying in the nanotube, and at points $2'$ and $3'$, lying in between the nanotubes. The data obtained can help one compare various theoretical approaches and determine the electron structure of the rope.

We have also performed the analyses of the angular distributions of 1 GeV protons transmitted through the 1 μm long ropes of (10, 0) and (5, 5) single-wall carbon nanotubes. These nanotubes are achiral too. In the former case each nanotube is defined by 20 atomic strings and in the latter case by 10 pairs of atomic strings. The angular distribution in the (10, 0) case is similar to the one in the (10, 10) case while the angular distribution in the (5, 5) case is very different from the one in the (10, 10) case. In both cases it is easy to make the correspondence between the parts of the angular distributions and the transverse lattice structures of the ropes. It should be also noted that the evolution of the angular distribution in the (10, 0) case with the proton energy or the rope length is different from the evolution in the (10, 10) case, enabling one to distinguish between the two types of ropes.

4 Conclusions

We have applied here the theory of crystal rainbows to the transmission of 1 GeV protons through the 1 μm long rope of (10, 10) single-wall carbon nanotubes. The analysis has shown that the angular distribution of transmitted protons contains the information on the transverse lattice structure of the rope. It has been also shown that the rainbow pattern determines the angular distribution and that all its pronounced maxima, except the maximum lying at the origin, can be attributed to the rainbow effect. These maxima can be used to measure the average electron density in the rope, i.e., in the nanotubes and in between them. Thus, our results could lead to a new method for characterization of achiral nanotubes, based on the rainbow effect. This method would be complementary to the existing method for characterization of nanotubes by electrons impinging on them transversely rather than longitudinally, which is based on the diffraction effect [17]. Besides, we think that our approach, enabling one to analyze and explain in detail the angular distributions of transmitted ions, can contribute considerably in clarifying and solving the problem of guiding of ion beams by nanotubes [5–8].

References

1. S. Iijima, Nature **354**, 56 (1991)
2. R. Saito, G. Dresselhaus, M.S. Dresselhaus, *Physical Properties of Carbon Nanotubes* (Imperial College Press, London, 2001)
3. Z. Yao, H.W.Ch. Postma, L. Balents, C. Dekker, Nature **402**, 273 (1999)
4. V.V. Klimov, V.S. Letokhov, Phys. Lett. A **222**, 424 (1996)
5. L.A. Gevorgian, K.A. Ispirian, R.K. Ispirian, Nucl. Instrum. Meth. Phys. Res. B **145**, 155 (1998)
6. N.K. Zhevago, V.I. Glebov, Phys. Lett. A **250**, 360 (1998); N.K. Zhevago, V.I. Glebov, Phys. Lett. A **310**, 301 (2003)
7. V.M. Biryukov, S. Bellucci, Phys. Lett. B **542**, 111 (2002); S. Bellucci, V.M. Biryukov, Yu.A. Chesnokov, V. Guidi, W. Scandale, Nucl. Instrum. Meth. Phys. Res. B **203**, 236 (2003)
8. A.A. Greenenko, N.F. Shulga, Nucl. Instrum. Meth. Phys. Res. B **205**, 767 (2003)
9. S. Petrović, L. Miletić, N. Nešković, Phys. Rev. B **61**, 184 (2000)
10. N. Nešković, S. Petrović, L. Živković, Eur. Phys. J. B **18**, 553 (2000)
11. N. Nešković, S. Petrović, D. Borka, S. Kossionides, Phys. Lett. A **304**, 114 (2002)
12. S. Petrović, S. Korica, M. Kokkoris, N. Nešković, Nucl. Instrum. Meth. Phys. Res. B **193**, 159 (2002)
13. A. Thess, R. Lee, P. Nikolaev, H. Dai, P. Petit, J. Robert, C. Xu, Y.H. Lee, S.G. Kim, A.G. Rinzler, D.T. Colbert, G. Scuseria, D. Tománek, J.E. Fischer, R.E. Smalley, Science **273**, 483 (1996)
14. J. Lindhard, K. Dan. Vidensk. Selsk., Mat.-Fys. Medd. **34**, No. 14, 1 (1965)
15. See, e.g., H.F. Krause, J.H. Barrett, S. Datz, P.F. Dittner, N.L. Jones, J. Gomez del Campo, C.R. Vane, Phys. Rev. A **49**, 283 (1994)
16. J. Hone, B. Batlogg, Z. Benes, A.T. Johnson, J.E. Fischer, Science **289**, 1730 (2000)
17. See, e.g., A.A. Lucas, F. Moreau, Ph. Lambin, Rev. Mod. Phys. **74**, 1 (2002)